Anisotropic model building with wells and horizons: Gulf of Mexico case study comparing different approaches

ANDREY BAKULIN, Saudi Aramco
YANGJUN (KEVIN) LIU, OLGA ZDRAVEVA, and KEVIN LYONS, WesternGeco

Anisotropic depth imaging with vertical transversely isotropic (VTI) models has become the dominant practice in the industry. However, anisotropic parameters for these models continue to be derived by basic practices without the use of tomography. Hanging a single profile of Thomsen's parameters from the water bottom still remains the most common practice. In a simple structural setting, it is usually possible to focus the data and obtain a good image despite having a simple and unrealistic model for Thomsen's parameters. However, depth positioning of such images is usually suboptimal. Better positioning requires more geologically plausible models. In addition, imaging in complex settings may require tilted transversely isotropic (TTI) models.

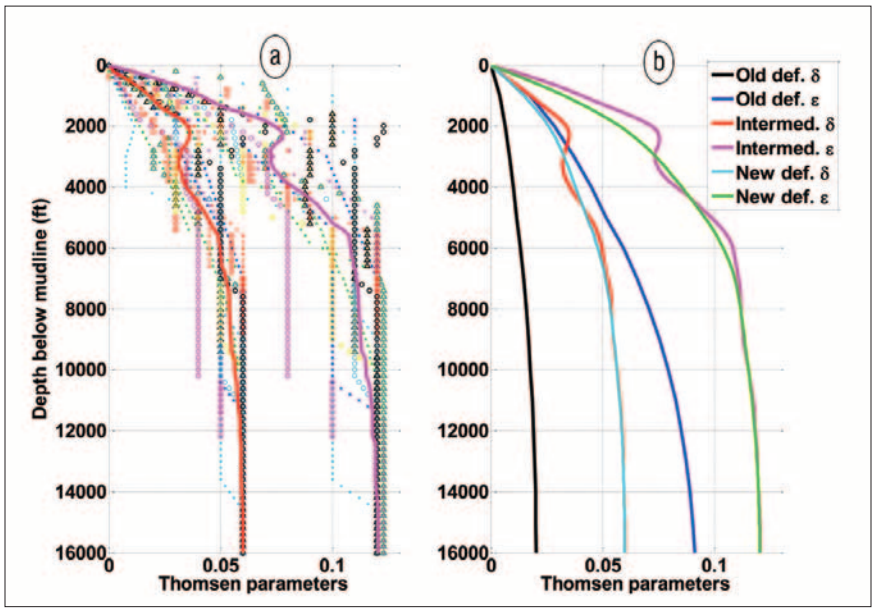

Figure 1. *(a) Profiles of Thomsen's parameters inverted at 18 well locations (various colors) together with their simple average (solid lines). (b) Profiles for scenarios 1-3: old default that uses no well calibration; intermediate is a slightly smoothed version of the average profiles from (a), whereas new default is a heavily smoothed version of the same profiles.*

In this case study, we construct several anisotropic models using approaches with increasing complexity and evaluate the model impact on image quality and ties to well data. We start with a "new default" model, where a single, smoothed, borehole-calibrated profile is hung from the water bottom, then progress to an "intermediate" model where a similar profile with more vertical details is propagated using major geological horizons. We finish with an "elaborate" model, where profiles from several wells are interpolated throughout the model using geologic horizons.

We contrast all models with an "old default" model derived without well calibration. We observe a generally steady improvement in well ties compared to the "old default" model, with the proportionally largest change coming from simple well calibration ("new default" model) and additional uplift coming from incorporating geologic horizons ("intermediate" model). Differences between intermediate and elaborate models are small, while switching to TTI models clearly helps to resolve complex structures in steeply dipping areas.

Case study from the Green Canyon area, Gulf of Mexico

It is well understood that seismic data do not constrain all parameters of an anisotropic velocity field (Tsvankin, 2001). Therefore, Thomsen's parameters are usually estimated by jointly using well and seismic data at borehole locations (Bear et al., 2005). Profiles derived at wells are extrapolated or interpolated throughout the volume and kept static, whereas velocity is updated with tomography. It is a general expectation that more accurate and geologically plausible volumes of models of Thomsen's parameters may lead to better images and improved well ties. We apply several different model-building practices and quantify their impact on imaging and ties to well data.

The area of interest is in the northern part of the Green Canyon area, U.S. Gulf of Mexico. Seismic data consist of 100 outer continental shelf (OCS) blocks of wide-azimuth acquisition. Well data consist of check-shot and wireline log data for 18 wells. We consider these five scenarios to derive Thomsen parameters ε and δ:

1) Old default VTI (A single, smooth regional profile is hung from the water bottom; no well calibration.)
2) New default VTI (A single, smoothed, borehole-calibrated profile is hung from the water bottom.)
3) Intermediate VTI (A single, borehole-calibrated profile is interpolated using seven major horizons.)
4) Elaborate VTI (Profiles of ε and δ from 18 wells are interpolated using seven major horizons.)
5) Elaborate TTI (The same Thomsen parameters as elaborate VTI, but symmetry axis is now perpendicular to bedding.)

In the first scenario, profiles of Thomsen's parameters plateau at ε = 0.09 and δ = 0.02, whereas, in the second and third scenarios, they plateau at ε = 0.12 and δ = 0.06 (Figure 1). At each of the 18 wells in the areas of small geologic dip, we have performed manual 1D layer-stripping inversion of seismic and check-shot data for Thomsen's parameters ε and δ

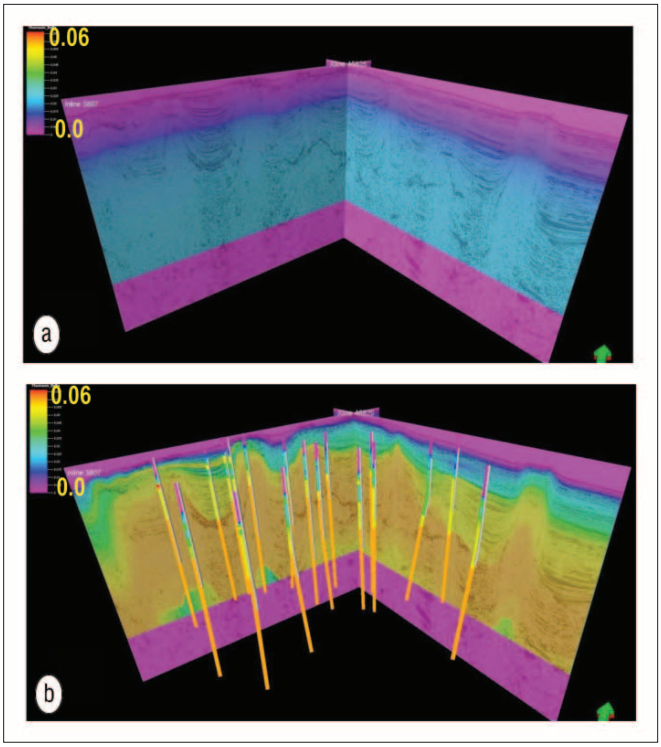

Figure 2. *Thomsen's δ volume for (a) old default VTI and (b) elaborate VTI models. Thomsen's δ profiles are shown along the tracks of 18 wells.*

as described by Bakulin et al. (2010). The intermediate profile is obtained by averaging these 18 profiles without smoothing, whereas the new default is obtained by averaging and smoothing (Figure 1). Smoothing removes high-frequency features that cannot be accurately propagated in the subsurface when only the water-bottom horizon is used for extrapolation.

Each model is constructed using a simple workflow (Bakulin et al., 2010) that consists of four major steps:

1) Derive local anisotropy profiles around existing wells.
2) Pick a set of key seismic horizons.
3) Populate volumes of anisotropic parameters using horizon-guided interpolation of anisotropic profiles derived at wells.
4) Update velocity along the symmetry axis with reflection tomography (without well constraints).

The first two VTI scenarios are special cases of this approach where only a single horizon (water bottom) is used for property extrapolation and anisotropy profiles are idealized. For the remaining scenarios in this study, anisotropy profiles at 18 wells were derived by 1D manual layer-stripping inversion (Bakulin et al., 2010). Sediment velocity was estimated from check-shot data and kept static, whereas the seismic gather at the well location was flattened by manually updating Thomsen's ε and δ profiles. In dipping areas or for deviated wells, one may also use local tomography to evaluate the local anisotropy model (Bakulin et al., 2009). Both 1D inversion and local tomography assume that anisotropy is slowly

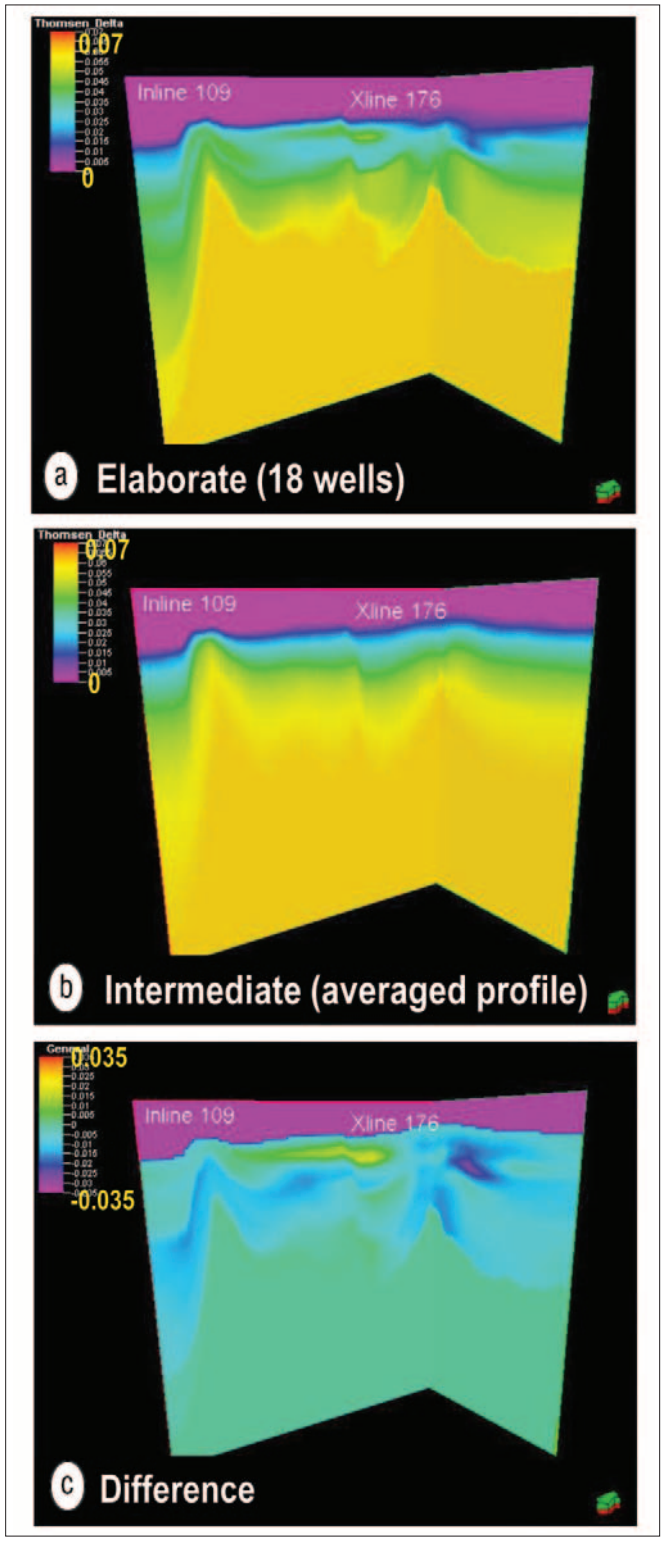

Figure 3. *Thomsen's δ volume for (a) elaborate VTI and (b) intermediate VTI models together with their difference (c). Observe the lateral change of anisotropy within layers in the elaborate VTI model caused by variability of Thomsen's δ profiles derived at the wells.*

varying along horizontal or dipping layers. Seven subsurface horizons were interpreted in the initial model (old default VTI) and then used in scenarios 3, 4, and 5 to guide the propagation of anisotropic properties between the wells. In

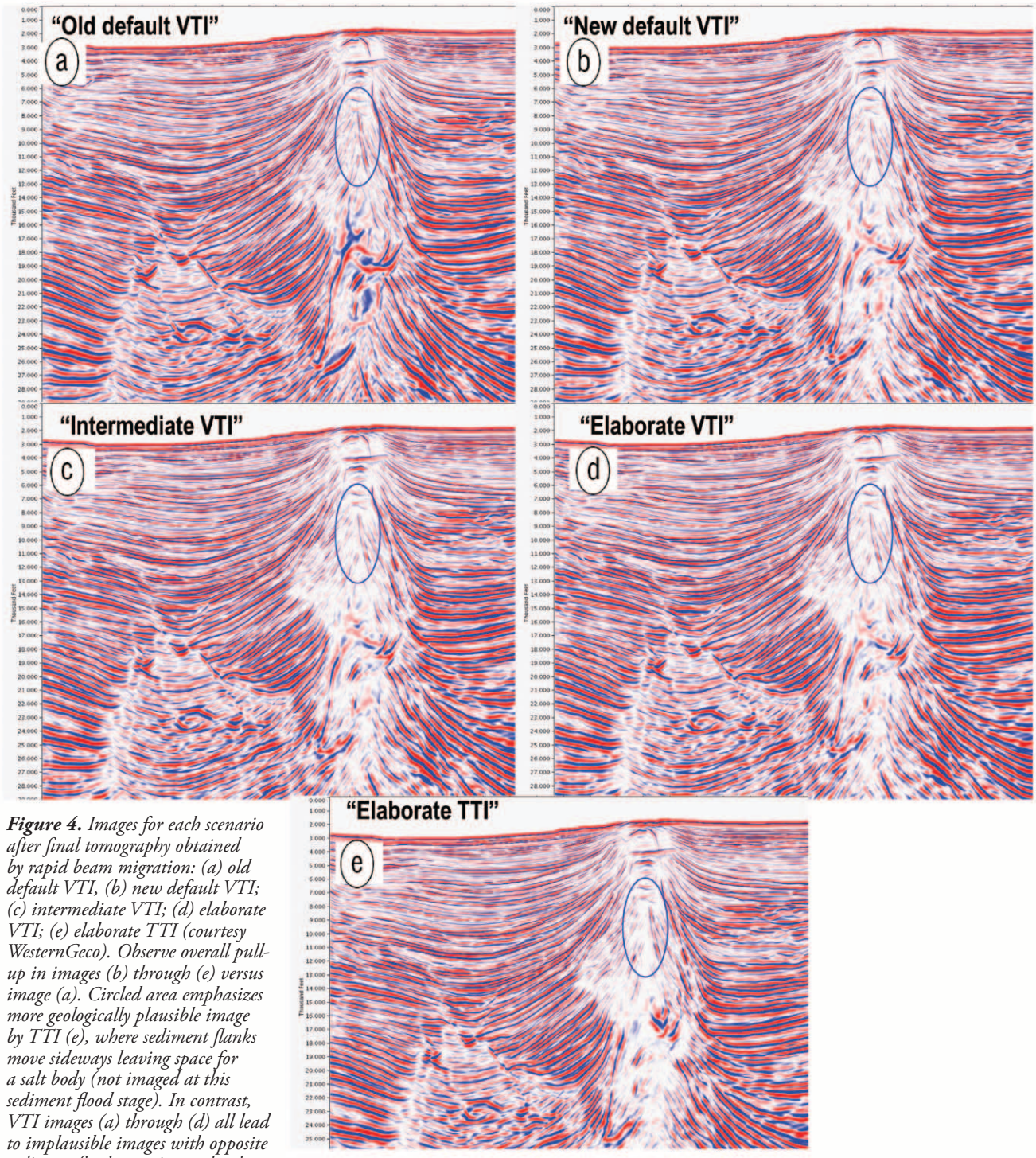

Figure 4. *Images for each scenario after final tomography obtained by rapid beam migration: (a) old default VTI, (b) new default VTI; (c) intermediate VTI; (d) elaborate VTI; (e) elaborate TTI (courtesy WesternGeco). Observe overall pull-up in images (b) through (e) versus image (a). Circled area emphasizes more geologically plausible image by TTI (e), where sediment flanks move sideways leaving space for a salt body (not imaged at this sediment flood stage). In contrast, VTI images (a) through (d) all lead to implausible images with opposite sediment flanks crossing each other. (Courtesy WesternGeco)*

each layer, except the deepest, both top and bottom horizons were used as interpolation guides. In scenarios 1 and 2, as well as for the deepest layer in scenarios 3, 4, and 5, only the top horizon was used as a guide, thus making property isosurfaces parallel to this horizon (Figure 2). Interpolating anisotropic parameters between the well consists of four substeps:

3.1) Convert profiles of Thomsen's parameters along the wells from well depth to seismic image depth.

3.2) Interpolate Thomsen's parameters between wells using horizons in seismic image depth.

3.3) Revise symmetry-axis velocity in a volume to maintain the same normal-moveout velocity.

3.4) Transform the entire velocity model into a new seismic image depth.

The first substep is required to bring the anisotropy profiles derived in well depth to seismic image depth where ho-

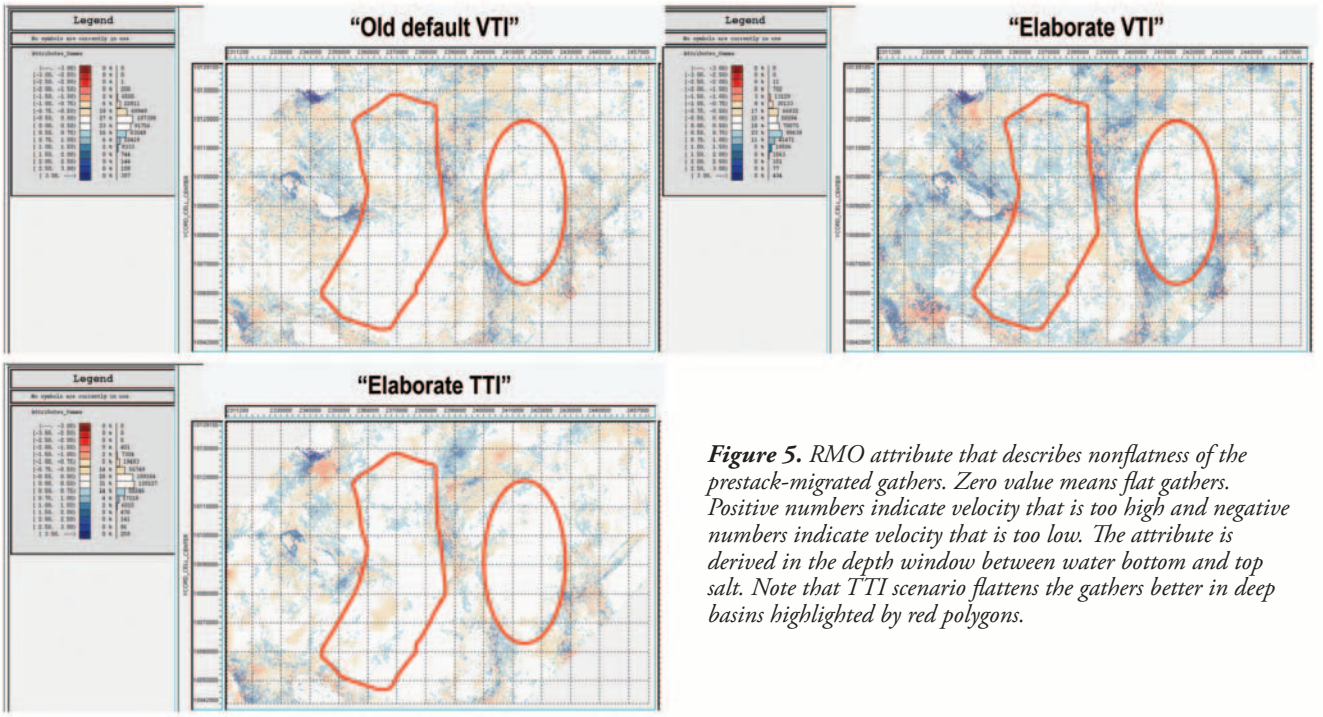

Figure 5. *RMO attribute that describes nonflatness of the prestack-migrated gathers. Zero value means flat gathers. Positive numbers indicate velocity that is too high and negative numbers indicate velocity that is too low. The attribute is derived in the depth window between water bottom and top salt. Note that TTI scenario flattens the gathers better in deep basins highlighted by red polygons.*

rizons are interpreted. To preserve interval normal moveout velocity after changing anisotropy volumes, we also update the vertical velocity at the third substep using the simple 1D VTI equation

$$V_{P0}^{new} = V_{P0}^{old}\sqrt{\frac{(1+2\delta^{old})}{(1+2\delta^{new})}}\,.$$

At well locations in a 1D VTI Earth, such a correction is expected to convert seismic velocity into well velocity while maintaining the same gather flatness. In laterally heterogeneous models, we expect seismic velocity to closely approach well velocity. This also facilitates quicker convergence for subsequent tomography iterations that only update symmetry-axis velocity. At the last substep, we convert the model into a new seismic image depth controlled by the revised seismic vertical velocity. This was accomplished using a simple 1D transform to time using the initial velocity, followed by conversion to depth using the revised seismic vertical velocity.

Figure 2 shows the impact of using subsurface horizons on anisotropy interpolation by contrasting Thomsen's δ volumes for the old default and elaborate models. In the old default model, anisotropy is low and varies conformably to the water bottom (Figure 2a). In contrast, the elaborate model has higher anisotropy that conforms to subsurface geology (Figure 2b). Figure 3 highlights the differences between the elaborate and intermediate models, which mainly result from lateral variation of anisotropy within layers caused by variability of anisotropy profiles at the well locations.

After generating the anisotropic volumes, anisotropic (VTI or TTI) tomography was run to update velocity along the symmetry axis (Woodward et al., 2008) and final images were produced.

We emphasize that in our workflow horizons are used for guiding the population of Thomsen's parameters as well as for assessing horizon/image movements caused by new anisotropy volumes. However, grid tomography, employed at the fourth step, does not explicitly use horizons. Tomography updates symmetry-axis velocity at each grid point of the entire sediment volume, whereas volumes of Thomsen's parameters (interpolated using horizons) are kept fixed. Of course, after each tomographic iteration, horizons are remigrated with a new anisotropic velocity model in order to properly reposition them and re-evaluate the well ties.

Impact on imaging and residual moveout

Figure 4 compares images for each of the five scenarios after the final iteration of tomography. Note that these migrations are done at the sediment flood stage of processing and, therefore, salt bodies are not well focused. All seismic events are shallower in Figures 4b through 4e than in Figure 4a because of the slower velocities induced by larger values of Thomsen's parameters. Images for all VTI scenarios have similar focusing and mainly differ by vertical positioning. Larger horizontal shifts occur for the TTI scenario, thus making anticline-type structures appear wider. This leads to more realistic images in areas of high dip where VTI scenarios suggest geologically implausible crossing structures. Highlighted areas in Figures 4a through 4d indicate that sediment flanks on both sides of the salt are touching each other and crossing in VTI images. In contrast, in the TTI image, opposite flanks spread apart and make a space for the salt body (Figure 4e).

Additional justification for better validity of the TTI scenario may be also seen in the behavior of residual moveout (RMO) of prestack-migrated data after the final iteration of tomography. Figure 5 compares RMO attributes for two VTI

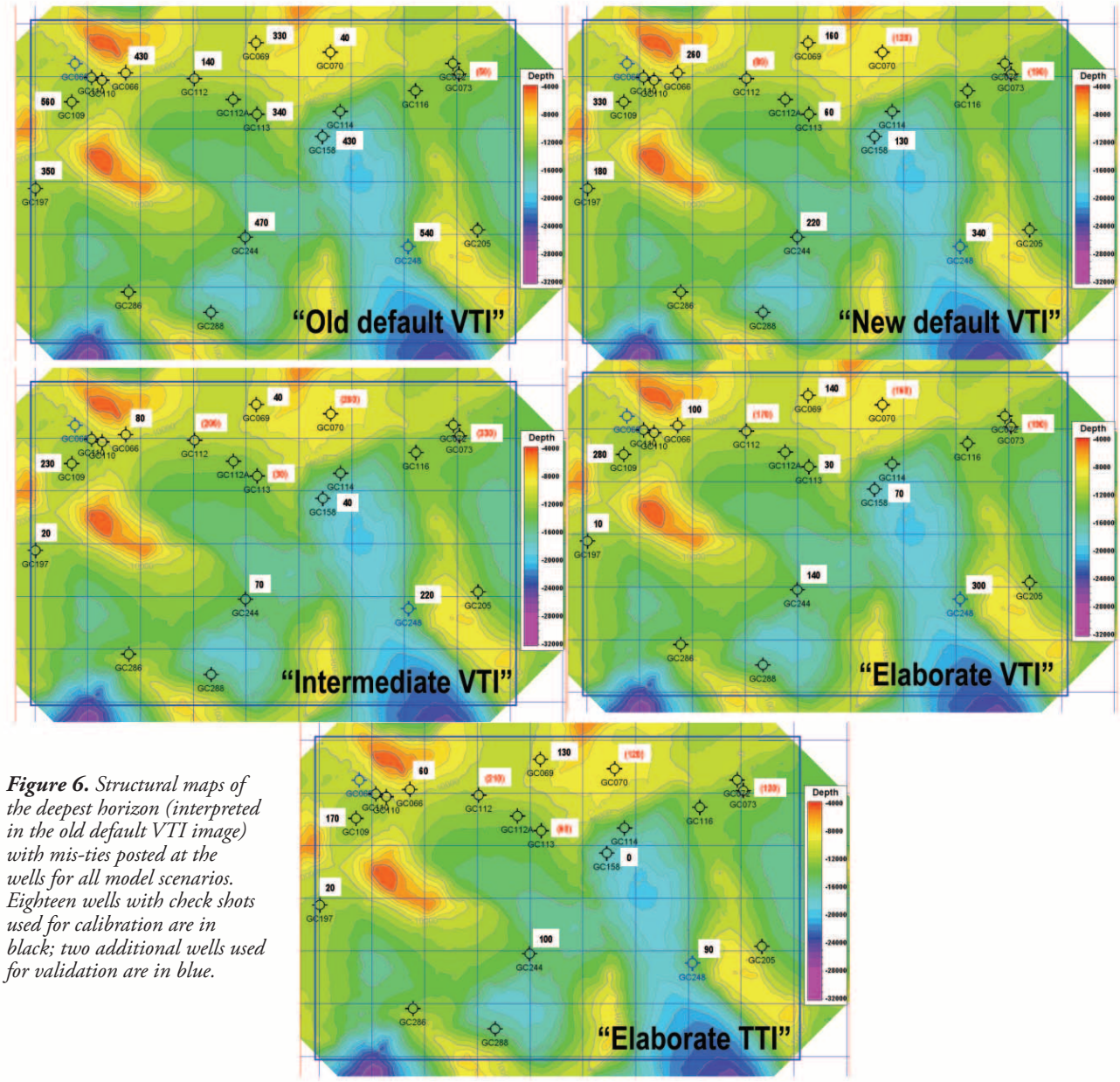

Figure 6. *Structural maps of the deepest horizon (interpreted in the old default VTI image) with mis-ties posted at the wells for all model scenarios. Eighteen wells with check shots used for calibration are in black; two additional wells used for validation are in blue.*

and one TTI scenarios. All three scenarios have very small residual moveout; however, in a statistical sense, the TTI model provides better flattening of the gathers in deep basins. For instance, the percentage of picks in two middle bands with an RMO error less than 0.5% is 50% for the old default VTI and 33% for the elaborate VTI, whereas it reaches the highest value of 59% for the elaborate TTI scenario.

Well mis-ties

To judge the positioning accuracy of different models, we evaluated mis-ties for 11 wells. Check shots from all except one (GC248) have been used for calibrating anisotropic models. Figure 6 shows a structural map of the deepest horizon used for anisotropy interpolation with corresponding values of the mis-ties for all model scenarios, whereas Figure 7 summarizes all the mis-tie values by model scenario. Eight out of 11 wells exhibit reduction in mis-ties as we progress from the old default VTI to more detailed borehole-calibrated models. While well GC248 has not been used in calibration, it also shows reduced mis-ties for new models. For wells in this category, a similar conclusion also applies to all shallow markers as shown in Figures 8 and 9. The largest improvement occurs when the simplest form of borehole calibration is introduced (i.e., when moving from old default VTI to new default VTI). While this improvement is huge, it is no longer representative of the current industry practice where all anisotropic parameters in initial models are based on some sort of well calibration from the area. The second biggest improvement occurs when we propagate a single (but more detailed) profile according to subsurface horizons (i.e., when moving from new default VTI to intermediate VTI). This improvement is more relevant to current prac-

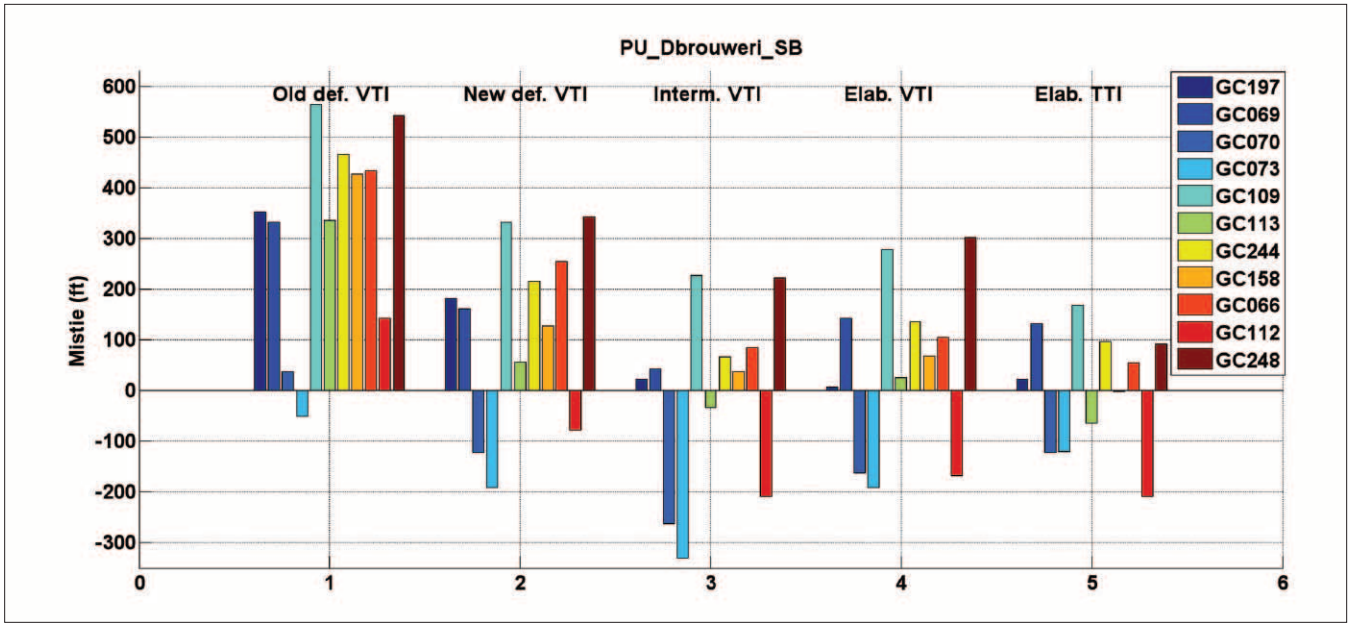

Figure 7. *Mis-tie at deepest horizon evaluated in this study for a collection of 11 wells from Green Canyon, shown for all five VTI and TTI model scenarios. Observe an overall decrease in mis-ties when moving to a more detailed subsurface model, except in the three northern outlier wells (GC070, GC073, and GC112).*

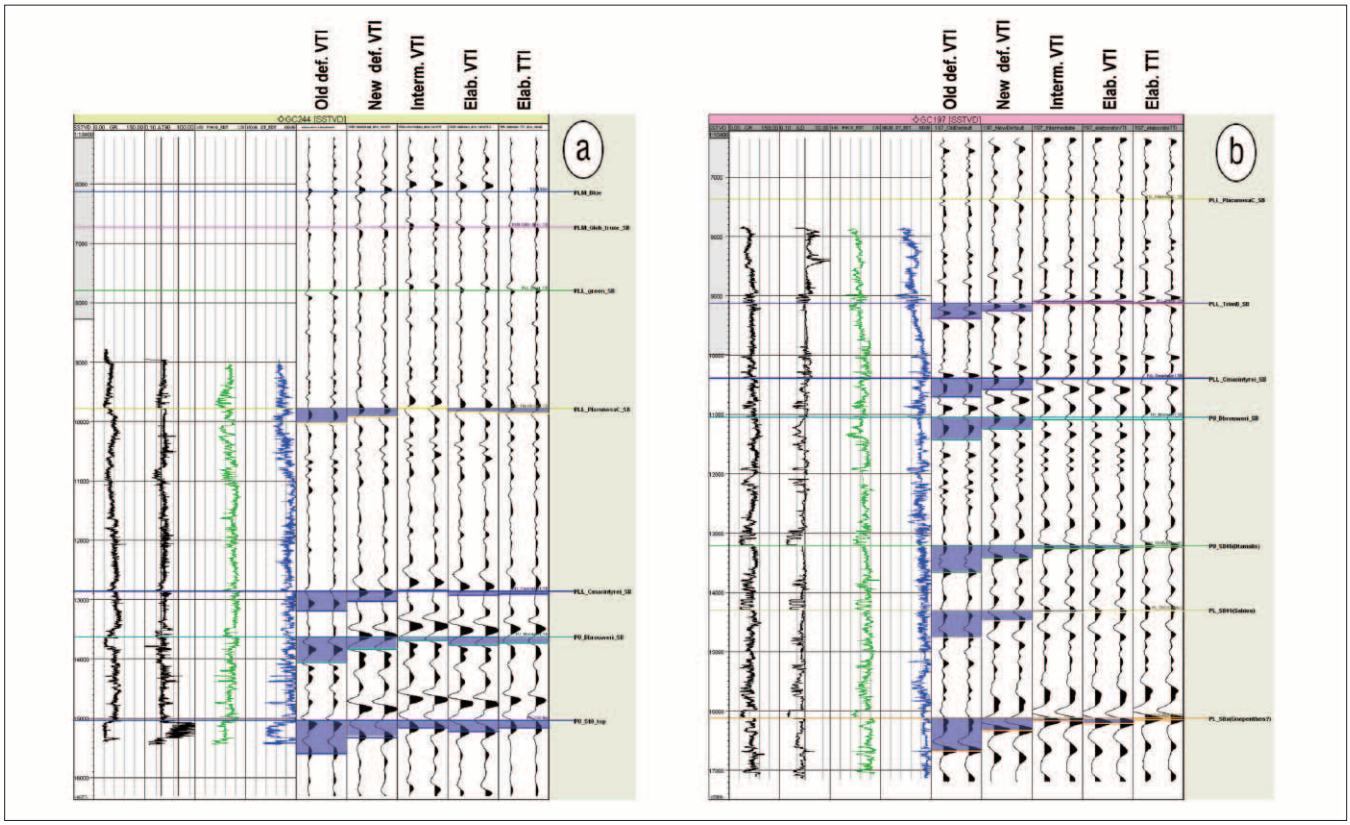

Figure 8. *Graphical representation of well mis-ties for two good wells where mis-ties improve in the new calibrated models. Corresponding stack traces from each image for five model scenarios are shown and mis-ties are color-coded: (a) well GC244 and (b) well GC197. Well-log data supplied by IHS Energy Log Services.*

tices that often consider this step as optional without fully understanding the consequences. Also, reduced mis-ties in the intermediate VTI model seem to validate the assumption that anisotropy is likely controlled by lithology (Bear et al.) and highlights the value of using subsurface horizons in model building. The elaborate VTI model is locally more accurate than intermediate VTI (Figure 9b), but not uniformly so and, in places, produces worse mis-ties (Figure 9a). Elaborate TTI seems to provide slightly better misfits than elaborate VTI (Figure 7), despite the fact that calibration lo-

cations are all areas of low dip. This is possibly a consequence of the fact that two iterations of tomography were run for the TTI scenario, whereas only a single iteration was performed for each VTI scenario.

While ties improve in the majority of the wells with increasing model complexity, it is clearly not the case for the outlier wells GC070, GC073, and GC112, where the best ties to well data are achieved with the old default VTI model. Figure 10 confirms that old default VTI provides the smallest mis-ties for all well markers for this group of wells. All wells are in the northern or northwestern part of the area, suggesting that possibly this region is somehow different from the rest in terms of rock properties.

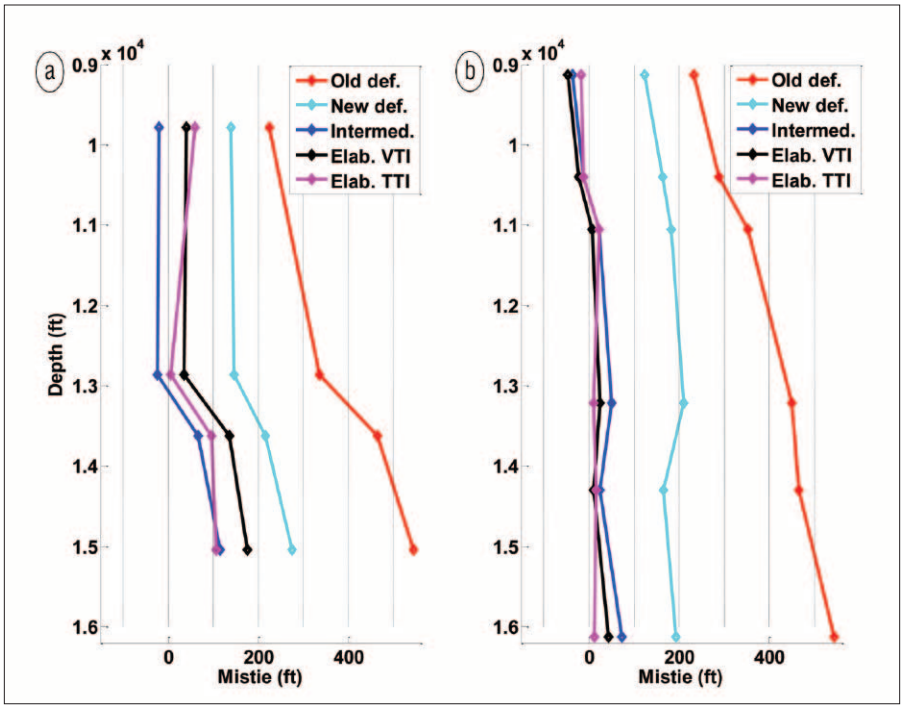

Figure 9. *Same as Figure 7 but well mis-ties are shown as a function of depth for VTI and TTI model scenarios after final tomography: (a) well GC244 and (b)well GC197.*

Validation with check shots

While the mis-tie analysis above is useful, it should always be taken with a grain of salt. Standard industry well-tie analysis is a highly interpretive process that relies on many assumptions that are often not satisfied in practice (Allouche et al., 2009). Therefore, it is quite instructive to analyze fits to the check-shot data as well. First-arrival traveltimes recorded in a borehole seismic survey represent a more robust data set that does not require much additional interpretation and, therefore, may have less ambiguity as compared to well-tie analysis. Nevertheless, there are other issues that may affect such a comparison and it is extremely important to keep them in mind. First, it is well known that in the deepwater Gulf of Mexico, water velocity varies with time (Carvill, 2009). Because borehole and surface seismic data are acquired at different times, often years apart, such differences can be up to 10 ms in 3000 ft of water. In addition, water velocity replacement schemes may further alter

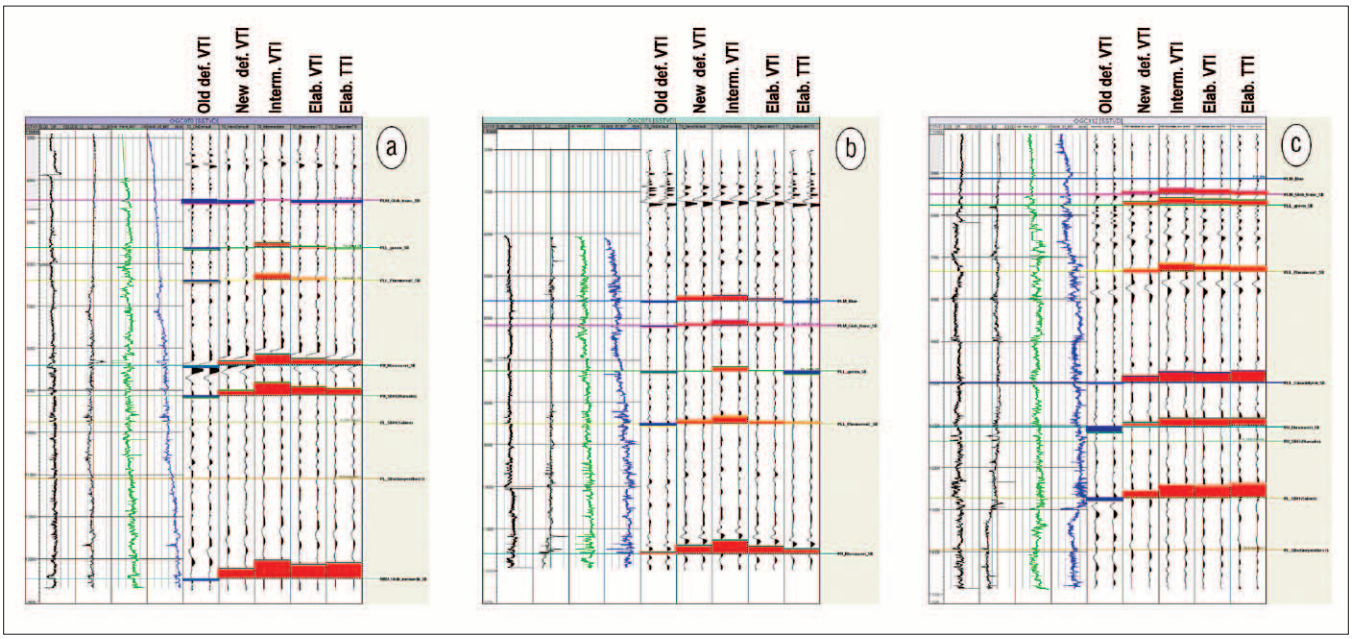

Figure 10. *Graphical representation of well mis-ties for three outlier wells where mis-ties deteriorate in the new calibrated models. Corresponding stack traces from each image for five model scenarios are shown and mis-ties are color-coded: (a) well GC070; (b) well GC073; and (c) well GC112. Well-log data supplied by IHS Energy Log Services.*

measured seismic traveltimes and drift them away from the borehole seismic data. As a result, it is difficult to compare first-arrival traveltimes ray-traced in a seismic velocity model with the traveltimes directly recorded in a borehole seismic survey without first accounting for these effects. To deal with this problem, in Figures 11 and 12, we have introduced a constant traveltime shift into the measured check-shot data so that the residual with the modeled traveltimes is zero at the water bottom.

Let us start with modeling traveltimes by ray tracing around good wells used for calibration where mis-ties improve when we go from old to new models. Figure 11 confirms that in such wells, fit to check-shot data also improves in more detailed models, although the progression of these improvements is slightly different than that observed for the mis-ties in the same set of wells (Figures 8 and 9). More independent validation comes from examining two wells (shown in blue in Figure 6) in more steeply dipping areas that have not been used for calibration. Dip changes from 7° at 4000 ft to 33° at 15,000 ft for the first well (Figure 12a), whereas, for the second, it is between 3° and 11° (Figure 12b). Again, we observe reductions in misfit when switching to borehole-calibrated models and adding horizons; however, elaborate VTI seems a little worse than simpler models such as intermediate VTI, which is consistent with the mis-tie analysis for well GC248 (Figure 7). Elaborate TTI is better than elaborate VTI for a well that penetrates sediments with higher dip (Figure 12a), but slightly worse for a well with smaller dips (Figure 12b).

As for outlier wells, they occurred because originally we did not believe that rapid lateral variation of anisotropy (Thomsen's δ varying from 2 to 6%) was plausible across such relatively short distances, especially between well GC112 and surrounding wells GC066, GC112A, GC069, and GC113 (Figure 6). Thus, we tried to impose higher anisotropy values (typical for the rest of the area) to these outlier wells during manual 1D inversion at wells. This assumption backfired during validation with markers (Figure 10) as well as with check shots.

Irrespective of how we come up with the new anisotropic scenarios, Thomsen parameter volumes were generated with the final profiles and frozen, whereas symmetry-axis velocity in all of them was updated by reflection tomography that flattened the gathers. It became clear that every VTI or TTI scenario with higher anisotropy at these locations eventually led to deteriorating well ties and check-shot misfits in two out of the three outlier wells, whereas in the third one (GC070) check-shot and marker data contradicted each other. As a result, we conclude that the combination of seismic and well data likely suggests that low anisotropy values close to the old default VTI may be appropriate to the areas around GC073 and GC112. If we accept this conclusion, then it is likely that there exists a significant lateral variation of anisotropy in the northern part of the area (Figure 6) creating pockets of low anisotropy. It may be consistent with an overall transition to lower anisotropy values in shallow-water areas of the Gulf of Mexico. A detailed rock physics study is required to explain this significant variation in seismic anisotropy.

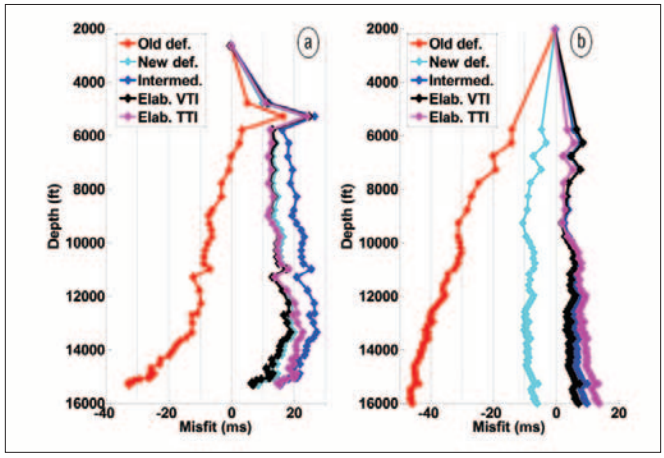

Figure 11. *Check-shot misfit for various VTI and TTI model scenarios after final tomography shown for two good wells that have been used in the calibration process: (a) GC244 and (b) GC197. Misfit is the difference between ray-traced in the model and experimental traveltimes.*

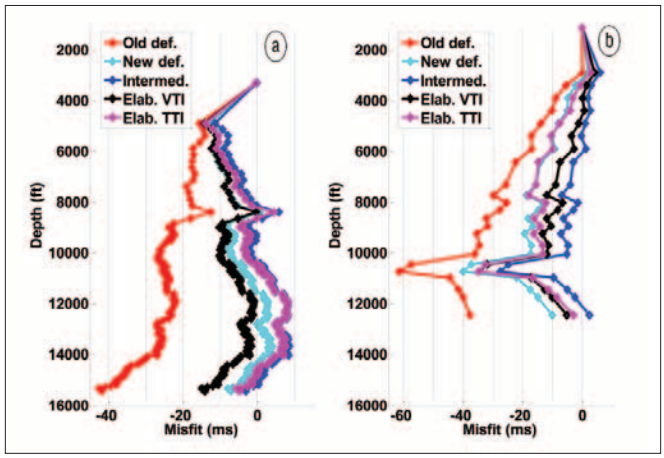

Figure 12. *Same as Figure 11 except for two vertical wells in the dipping areas that have not been used for calibration: (a) GC248 and (b) GC065.*

Movement of top salt horizon between various scenarios

While quantifying ties at selected well locations represents validation at sparse points, it is also of interest to review the depth movements of entire horizons between images produced using various model scenarios. We examine such displacements using zero-offset anisotropic map migration. Figure 13 quantifies movement of the top salt horizon between old default VTI and elaborate VTI. The mean value of the upward movement is about 400 ft (Figure 13b). The upward movement increases with increasing depth of the horizon (Figure 13c), and areas of high dip often exhibit anomalously large vertical displacement due to additional small lateral movements as explained in Figure 13d. If we quantify movement of top salt in other scenarios with respect to the elaborate VTI model, we generally observe significantly smaller displacements (Figure 14) than we see in Figure 13. Such displays may allow one to decide which model-building strategy is appropriate for each particular case. For instance, knowing that new default VTI and elaborate VTI only differ

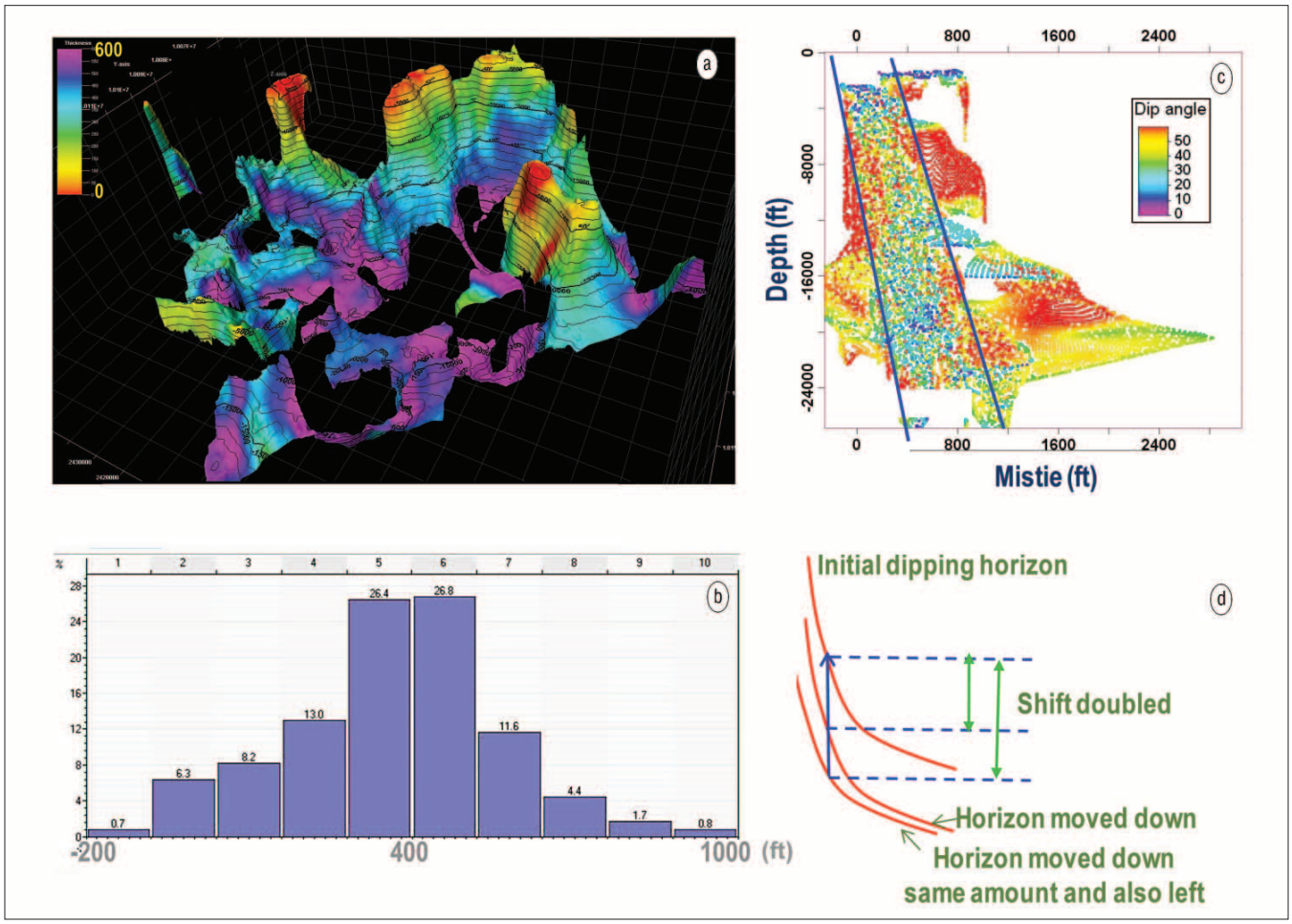

Figure 13. *Difference (mis-tie) locations of top salt horizon in two images generated with old default VTI and elaborate VTI models after final tomography: (a) difference (in ft) painted as an attribute on top of the salt horizon; (b) histogram of the difference; (c) difference as a function of depth color-coded by dip angle of the top salt horizon; and (d) cartoon explaining why larger displacement is expected in areas of higher dip. Positive displacement corresponds to shallower depth of top salt in elaborate VTI.*

by at most ±200 ft may justify using a new default for exploration projects, while reserving intermediate or elaborate models for development projects.

Discussion and conclusions

We have compared several approaches to building anisotropic VTI and TTI models. These approaches range from no well calibration, to using a single, borehole-calibrated profile, to the use of multiple well profiles. To propagate anisotropic parameters into the volume, we have used the water-bottom horizon in simple cases and seven geologic horizons in the most detailed cases. We have observed that the incrementally largest improvement in ties to well data comes from using a smoothed, single borehole-calibrated profile, even though it is still hung from the water bottom (new default VTI). Because currently industry uses some kind of well calibration on almost every survey, this represents a comparison of current and old industry practices. Smaller, yet substantial improvement occurs when subsurface horizons are used for propagation of Thomsen's parameters throughout the volume (intermediate VTI). Even though the intermediate model is still based on a single, borehole-calibrated profile, albeit with additional vertical detail, it produces reduced well mis-ties and provides a better fit to check-shot traveltimes compared to the new default VTI model. This conclusion validates the assumption that anisotropy is controlled by lithology and suggests that accurate well ties (within 100 ft) are unlikely to be achieved without using subsurface horizons in model building. Interestingly, the most detailed elaborate VTI model, where 18 profiles are interpolated using horizons, does not result in consistent improvement in mis-ties compared to the intermediate VTI model. More detailed investigation showed that the northern part of the Green Canyon study area may indeed have lower values of anisotropy, closer to the old default VTI that was originally dismissed. If we had allowed for strong, localized lateral variation in anisotropy as originally suggested by the data, then the elaborate VTI model would likely have produced significantly lower mis-ties in the northern outlier wells and, thus, would easily beat intermediate VTI that relied on a single averaged profile across the entire area.

The elaborate TTI scenario with symmetry axis perpendicular to bedding, on average, seems to have a slightly better fit to well data than does elaborate VTI, along with produc-

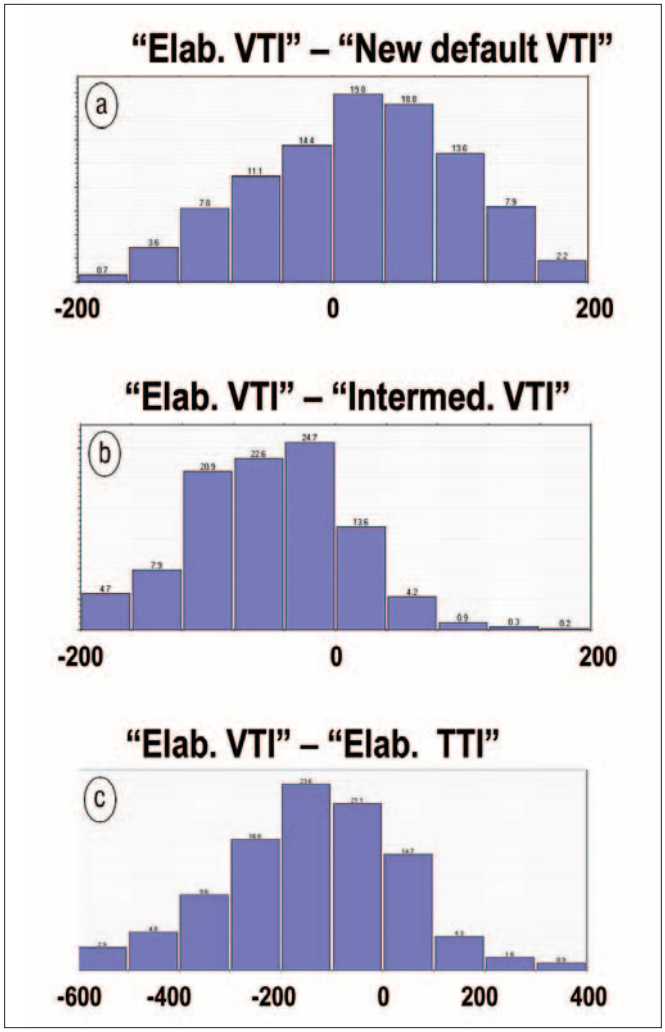

Figure 14. *Histogram of the difference (in ft) between locations of top salt horizon in elaborate VTI image and three other images obtained with different model scenarios. A positive number means that top salt in the elaborate VTI case is shallower than in the other scenario of interest.*

ing more geologically plausible images for steeply dipping anticline structures. Therefore, incorporating TTI anisotropy seems a logical next step for Gulf of Mexico surveys. Additional validation of this conclusion requires analyzing the impact of TTI models on subsalt imaging, which will be reported in subsequent studies. Finally, we note that even the best models do not guarantee achieving a certain predefined fit to well data. The described approaches utilize well data only at the onset when deriving anisotropic parameters near wells. Once the anisotropic parameters are determined, well data are no longer considered and reflection tomography only inverts seismic data for symmetry-axis velocity. There is no guarantee that updated velocity will lead to a good match of well data, unless volumes of Thomsen's parameters are perfect. Because our inversions for anisotropy are imperfect and almost always have large uncertainty (Bakulin et al., 2009), such a task is not achievable with a standard workflow as described in this study. Further improvement in the fit-to-well data would require additional tomography that jointly inverts seismic and well data, and perturbs both velocity and Thomsen's parameters. Alternatively, tomography with uncertainty (Bakulin et al., 2009) can be used to find nearby models from null-space that provide a better fit to well data, while keeping seismic gathers flat. Both approaches allow the correction of inaccuracies in the initial estimation of anisotropic parameters by slight perturbation of anisotropic parameters in the final stages of the model building. Nevertheless, these approaches do not completely replace calibration techniques described in this study, as their success usually requires an input anisotropic model that is close to the final state. Therefore, it is likely that, in practice, a two-step approach would be needed to achieve an objective of a certain predefined fit to well data. First, perform calibration as described in this study to get reasonably close to satisfying the well data; and second, fine-tune the constructed models to achieve the desired fit to well data by slight perturbation of anisotropy and velocity directly using well data again. Applying this two-step practical approach should still allow for reasonable project turnaround time, while also avoiding the generation of unrealistic bullseyes in anisotropic parameters within the model. TLE

References

Allouche, H., P. Thore, and T. Monnerie, 2009, Towards a better seismic to well tie in complex media: 79th Annual International Meeting, SEG, Expanded Abstracts, 1870–1874.

Bakulin, A., Y. Liu, and O. Zdraveva, 2010, Borehole-calibrated and geologically plausible anisotropic models using wells and horizon-guided interpolation: 72nd EAGE Conference and Exhibition, Extended Abstracts, C038.

Bakulin, A., M. Woodward, D. Nichols, K. Osypov, and O. Zdraveva, 2009, Anisotropic model building with uncertainty analysis: 79th Annual International Meeting, SEG, Expanded Abstracts, 3720–3724.

Bear, L. K., T. A. Dickens, J. R. Krebs, J. Liu, and P. Traynin, 2005, Integrated velocity model estimation for improved positioning with anisotropic PSDM: The Leading Edge, **24**, 622–634.

Carvill, C. V., 2009, A new approach to water velocity estimation and correction: 71st EAGE Conference and Exhibition, Extended Abstracts, U027.

Tsvankin, I., 2001, Seismic signatures and analysis of reflection data in anisotropic media. Elsevier Science, Elsevier.

Woodward, M., D. Nichols, O. Zdraveva, P. Whitfield, and T. Johns, 2008, A decade of tomography: Geophysics, **73**, no. 5, VE5–VE11.

Acknowledgments: We thank Kelvin Soice and Peter Wang (WesternGeco) for assistance with this study. We express our gratitude to Rick Kania and Robert Hubbard (WesternGeco) for sponsorship and encouragement. We thank Dave Nichols and Konstantin Osypov for supporting this study. We are grateful to WesternGeco for providing wide-azimuth seismic data for this study and was Andrey Bakulin's employer when the work was done. This work includes data owned by IHS Energy Log Services, Inc.

Corresponding author: a_bakulin@yahoo.com